Energetics and Mechanism of Alkylamine N−H Bond Cleavage by Palladium Hydroxides: N−H Activation by Unusual Acid−Base Chemistry

Michael S. Driver and John F. Hartwig*

Department of Chemistry, Yale University, P.O. Box 208107, New Haven, Connecticut 06520-8107

Received October 2, 1997[⊗]

The dimeric palladium hydroxide complex $[(PPh_3)(Ph)Pd(\mu\text{-}OH)]_2$ underwent proton exchange reactions to cleave the N−H bonds of both alkyl and aryl primary amines to generate dimeric palladium amido complexes. This acid−base chemistry was reversible and provided thermodynamic information on the relative bond energies of the bridging amido and bridging hydroxo ligands. The mechanism of the N−H activation reaction was studied in both the forward and reverse directions to gain a detailed picture of the reaction pathway. Our data indicate that the reaction proceeds via cleavage of the hydroxide dimer by association of 2 equiv of amine followed by reversible proton transfer to create the amido ligand and a bound water ligand. Reassociation of the amido monomer with one of the original hydroxide monomers with displacement of water and amine gives the final amido hydroxo dimer product. Microscopic reversibility leads to the prediction that the reaction of water with the amido complexes is first order in product amine and is, therefore, autocatalytic. This unusual kinetic behavior was observed.

Introduction

The catalytic chemistry of soluble transition metal complexes with alkylamine substrates is not well-developed.[1] One reason for this scarcity of catalysis with amines is the absence of reactive transition metal amido complexes prepared directly from alkylamine substrates. N−H bond cleavage processes that generate metal amido complexes are well-known for early transition metal complexes,[2,3] for alkali metals,[4−6] and for organolithium reagents.[4,6] However, early transition metal amides are often very stable, and alkali metal reagents are rare as catalysts.

The only soluble late transition metal complexes that cleave the NH bonds in alkylamines to form an amido complex by any reaction have involved Os clusters.[7−9] Even the oxidative addition of the NH bond of ammonia to late transition metal complexes is rare.[10] Despite the paucity of isolated amido complexes, they can act as viable intermediates in catalysis and are, most likely, intermediates in imine[11−29] and nitrile[30,31] hydrogenations, the amination of olefins,[32] and recently reported aryl halide aminations.[33−37]

The acid−base chemistry of alkali metal amides has been studied by a number of groups and is fundamental

⊗ Abstract published in *Advance ACS Abstracts,* December 1, 1997.

(1) Roundhill, D. M. *Chem. Rev.* **1992**, *92*, 1−27.
(2) Hillhouse, G. L.; Bercaw, J. E. *J. Am. Chem. Soc.* **1984**, *106*, 5472.
(3) Walsh, P. J.; Hollander, F. J.; Bergman, R. G. *Organometallics* **1993**, *12*, 3705−3723.
(4) Volhardt, K. P. C. *Organic Chemistry*; W. H. Freeman & Company: New York, 1987.
(5) Hancock, E. M.; Cope, A. C. *Organic Syntheses* **1945**, *25*, 25.
(6) Heaney, H. *Chem. Rev.* **1962**, *62*, 81−97 and references therein.
(7) Lin, Y.; Mayr, A.; Knobler, C. B.; Kaesz, H. D. *J. Organomet. Chem.* **1984**, *272*, 207−229.
(8) Bryan, E. G.; Johnson, B. F. G.; Lewis, J. *J. Chem. Soc., Dalton Trans.* **1977**, 1328−1330.
(9) The following paper includes the N−H activation of benzylamine, but the other amines in this work are arylamines, see: Glueck, D. S.; Winslow, L. J.; Bergman, R. G. *Organometallics* **1991**, *10*, 1462−1479.
(10) Casalnuovo, A. L.; Calabrese, J. C.; Milstein, D. *Inorg. Chem.* **1987**, *26*, 971−973.
(11) Amrani, Y.; Lecomte, L.; Simou, D.; Bakos, J.; Toth, I.; Heil, B. *Organometallics* **1989**, *8*, 542.
(12) Bakos, J.; Toty, I.; Heil, B.; Marko, L. *J. Organomet. Chem.* **1985**, *279*, 23.
(13) Bakos, J.; Toth, I.; Heil, B.; Szalontai, G.; Parkanyi, L.; Fulop, V. *J. Organomet. Chem.* **1989**, *370*, 263.
(14) Bakos, J.; Orosz, A.; Heil, B.; Laghmari, M.; Lhoste, P.; Sinou, D. *J. Chem. Soc., Chem. Commun.* **1991**, 1684.
(15) Becalski, A. G.; Cullen, W. R.; Fryzuk, M. D.; James, B. R.; Kang, G. J.; Rettig, S. J. *Inorg. Chem.* **1991**, *30*, 5002−5008.
(16) Burk, M. J.; Feaster, J. E. *J. Am. Chem. Soc.* **1992**, *114*, 6266.
(17) Chan, Y. N. C.; Osborn, J. A. *J. Am. Chem. Soc.* **1990**, *112*, 9400.
(18) Cullen, W. R.; Fryzuk, M. D.; James, B. R.; Kutney, J. P.; Kang, G. J.; Herb, G.; Thorburn, I. S.; Spogliarich, R. *J. Mol. Catal.* **1990**, *62*, 243.
(19) Imine hydrogenation catalyzed by rhodium and iridium complexes would be expected to occur through an amide complex. However, mechanistic data is scarce. For a direct observation of imine insertion that produces an amide complex potentially similar to those in catalytic systems, see: Fryzuk, M. D.; Piers, W. E. *Organometallics* **1990**, *9*, 986−98.
(20) For a recent review, see: James, B. R. *Chem. Ind.* **1995**, *62*, 167−180.
(21) Kang, G. J.; Cullen, W. R.; Fryzuk, M. D.; James, B. R.; Kutney, J. P. *J. Chem Soc., Chem. Commun.* **1988**, 1466.
(22) Longley, C. J.; Goodwin, T. J.; Wilkinson, G. *Polyhedron* **1986**, *5*, 1625.
(23) Ng, Y.; Chan, C.; Meyer, D.; Osborm, J. A. *J. Chem. Soc.m Chem. Commun.* **1990**, 869.
(24) Spindler, F.; Pugin, B.; Blaser, H. U. *Angew. Chem., Int. Ed. Engl.* **1990**, *29*, 558.
(25) Vastag, S.; Bakos, J.; Toros, S.; Takach, N. E.; King, R. B.; Heil, B.; Marko, L. *J. Mol. Catal.* **1984**, *22*, 283.
(26) Willoughby, C. A.; Buchwald, S. L. *J. Am. Chem. Soc.* **1992**, *114*, 7562.
(27) Willoughby, C. A.; Buchwald, S. L. *J. Org. Chem.* **1993**, *58*, 7627.
(28) Willoughby, C. A.; Buchwald, S. L. *J. Am. Chem. Soc.* **1994**, *116*, 11703−11714.
(29) Willoughby, C. A.; Buchwald, S. L. *J. Am. Chem. Soc.* **1994**, *116*, 8952.
(30) Armor, J. N. *Inorg. Chem.* **1978**, *17*, 203−213.
(31) Yoshida, T.; Okano, T.; Otsuka, S. *J. Chem. Soc., Chem. Commun.* **1979**, 870.
(32) Casalnuovo, A. L.; Calabrese, J. C.; Milstein, D. *J. Am. Chem. Soc.* **1988**, *110*, 6738−6744.

S0276-7333(97)00856-X CCC: $14.00

Scheme 1

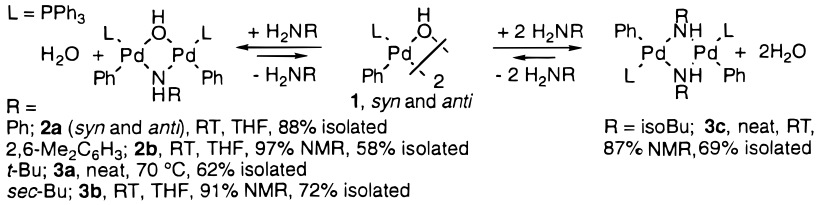

to many organic reactions.[6,38,39] The identity of the solvent and alkali metal has a large effect on the aggregation number and the resulting basicity. In contrast, the acid−base chemistry of late transition metal complexes with alkylamines and the acid−base chemistry of late transition metal alkylamides is much less explored. Since it is well-known that the identity of the metal can influence the basicity of a polar reagent, it is important to understand how the late transition metals and their accompanying ligands affect the acid−base chemistry of the amido group. It is this type of information that will assist in developing transition metal catalyzed chemistry involving amido groups and amine substrates such as arylation of amines, oxidation of amines, and formation of amines by hydrogenation.

We report here the unusual chemistry of hydroxide and alkylamide complexes of palladium toward alkylamines and water. Amines are deprotonated by palladium hydroxide complexes to form palladium amides. This reaction is, of course, exactly the opposite of what occurs with alkali metal reagents. Thus, the ion-pair acidity of alkylamines is, at least formally, greater than that of water in THF solvent when palladium is the counterion bound to the amide or hydroxide. A detailed account of the thermodynamics of this acid−base chemistry and of the mechanism by which the N−H bond is cleaved is reported, and it shows an unusual dependence of the rate on amine concentration in the forward direction and autocatalytic behavior in amine for the reverse.

Results

Palladium Amido Complexes by NH Bond Cleavage: Reactions of 1 with Primary Amines. The addition of excess primary amines to the PPh_3-ligated palladium aryl hydroxide dimer **1**[40,41] led to the complete consumption of **1**, elimination of water, and formation of palladium amides at either room temperature or slightly above room temperature in 58−88% isolated yields as outlined in Scheme 1. The reactions occurred in 68−97% yields by ^{31}P NMR spectrometry, with an internal standard, even for amines that generate palladium amides with β-hydrogens.

Complex **2a** was formed as a mixture of *syn*- and *anti*-isomers. Hydroxo dimer **1** is also a mixture of *syn*- and *anti*-isomers. The two isomers of **2a** were detected by ^{31}P and ^{1}H NMR spectroscopy. At room temperature, the ratio of the *syn*- and *anti*-isomers was approximately 1:2. The ratio of *syn*-isomer increased as a THF solution of **2a** was cooled, and crystallization from THF/Et_2O at −25 °C gave crystals of **2a** as predominantly (>90%) the *syn*-isomer. After several hours in aromatic solvents, a 1:2 equilibrium mixture of the two isomers was reestablished. Crystalline **2a** isomerized to an equilibrium mixture of isomers within 5 min at −20 °C in methylene chloride or THF. In contrast, only the *syn*-isomer that contained both phosphine ligands trans to the anilido group was observed for 2,6-dimethylanilide, **2b**.

Reaction of **1** in neat isobutylamine at room temperature for 15 min gave bis(amide) **3c**. Apparently, branching at the β-position gives mono(amido) complexes, but branching at the γ-position gives bis(amides). Reaction of 1 equiv of isobutylamine converted only half of the starting material **1** to the amide **3c**. No mixed palladium isobutylamido hydroxo dimer was observed. It was not necessary to use neat amine to observe complete conversion of **1**, but high amine concentrations reduced the formation of side products. The mixed dimers **3a** and **3b** possessed a *syn* geometry with the phosphine ligands trans to the amido group, while the bis(amido) dimer **3c** had an *anti*-geometry. The geometry of these complexes was determined by ^{1}H, ^{13}C, and ^{31}P NMR spectroscopy as well as X-ray diffraction in the case of **3a**.

Reaction of 1 with Secondary Amines. Reactions of **1** with secondary alkyl- or arylamines did not result in the formation of isolable palladium amido complexes. Reaction of 10 equiv of diethylamine with a THF solution of **1** at 70 °C or reaction in neat diethylamine at room temperature gave PPh_3O as the only product observed by ^{31}P NMR spectroscopy along with a black Pd-containing precipitate. Reaction of **1** with either diisopropylamine or *N*-methylaniline resulted in similar decomposition of **1** forming PPh_3O and a black Pd precipitate.

Reaction of 1 with Pyrrole. The addition of 5 equiv of pyrrole to a THF solution of **1** containing excess PPh_3 formed the monomeric palladium pyrrolyl complex *trans*-$(PPh_3)_2Pd(Ph)(NC_4H_4)$ (**4**), as shown in Scheme 2, in 91% isolated yield. The identity of this complex was confirmed by preparing it independently from KNC_4H_4 and *trans*-$(PPh_3)_2Pd(Ph)I$.

Reaction of Thiol To Form Palladium Thiolato Complexes. As expected, the more acidic SH bond of thiols also reacted with the dimeric palladium hydroxides to generate palladium thiolato complexes. As shown in Scheme 2, reaction between 2.5 equiv of *tert*-butylthiol and tolylpalladium hydroxo complex **1b** at room temperature formed the bis(thiolato)palladium complex **5** in 49% isolated yield. Comparison of the ^{1}H

(33) Louie, J.; Hartwig, J. F. *Tetrahedron Lett.* **1995**, *36*, 3609.
(34) Guram, A. S.; Rennels, R. A.; Buchwald, S. L. *Angew. Chem., Int. Ed. Engl.* **1995**, *34*, 1348.
(35) Louie, J.; Paul, F.; Hartwig, J. F. *Organometallics* **1996**, *15*, 2794−2805.
(36) Driver, M. S.; Hartwig, J. F. *J. Am. Chem. Soc* **1996**, *118*, 7217−7218.
(37) Wolfe, J. P.; Wagaw, S.; Buchwald, S. L. *J. Am. Chem. Soc.* **1996**, *118*, 7215−7216.
(38) Gregory, K.; Schleyer, P. v. R.; Snaith, R. *Adv. Inorg. Chem.* **1991**, *37*, 47 and references therein.
(39) Collum, D. B. *Acc. Chem. Res.* **1993**, *26*, 227−234 and references therein.
(40) Gurshin, V. V.; Alper, H. *Organometallics* **1993**, *12*, 1890−1901.
(41) We have modified the procedure for the synthesis of **1** as described in the Experimental Section.

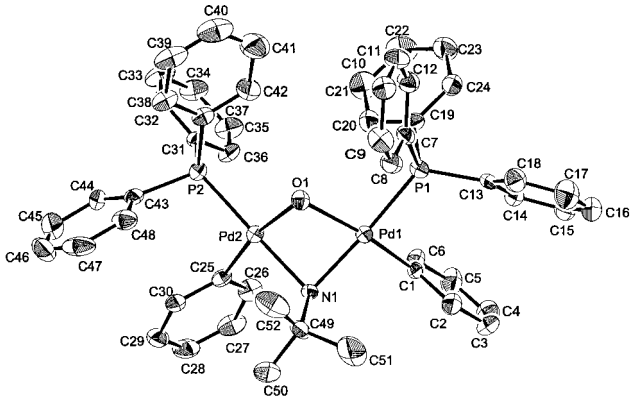

Figure 1. ORTEP drawing of $\{Pd_2(PPh_3)_2Ph_2(\mu\text{-OH})(\mu\text{-NH-}t\text{-Bu})\}$(**3a**). Hydrogen atoms are omitted for clarity.

Scheme 2

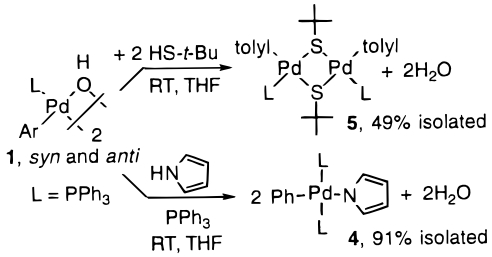

Table 1. Data for X-ray Structure of $\{Pd_2(PPh_3)_2Ph_2(\mu\text{-OH})(\mu\text{-NH-}t\text{-Bu})\}$ (3a)

empirical formula	$C_{52}H_{51}N_1O_1P_2Pd_2 \cdot C_{2.6}H_{1.6}Cl_{1.6}$
fw	1070.29
cryst color/habit	colorless plate
cryst syst	triclinic
lattice params:	
	$a = 12.765(3)$ Å
	$b = 14.029(5)$ Å
	$c = 15.176(4)$ Å
	$\alpha = 94.65(2)°$
	$\beta = 107.81(2)°$
	$\gamma = 93.30(2)°$
volume	2569(3) Å^3
space group	$P\bar{1}$ (No. 2)
Z value	2
radiation	Mo Kα ($\lambda = 0.710\ 69$ Å)
temperature	−93 °C
residuals: R, R_w	0.040; 0.056
goodness of fit indicator	3.16

and ^{31}P NMR spectra of **5** to previously prepared palladium thiolato dimers[42] confirmed the identity of **5** and indicated that the complex has a *syn*-geometry.

Reaction of 1 with Alcohols and Peroxides. Reaction between **1** and alcohols or peroxides did not provide clean chemistry. No reaction between **1** and either *tert*-butyl alcohol or *tert*-butyl hydroperoxide occurred at room temperature, while reaction at 70 °C for 2 h gave a black Pd precipitate and PPh_3O.

X-ray Crystal Structure of 3a. An X-ray quality crystal of **3a** was obtained by slow crystallization from CH_2Cl_2/Et_2O at −35 °C. An ORTEP diagram of **3a** is provided in Figure 1 with selected distances (Å) and angles (deg) given in Tables 2 and 3.[43] The four-membered ring core is markedly puckered. The dihedral angle between the O−Pd1−N and O−Pd2−N planes is 56.91°. As discussed recently,[44] some bridging hydroxo and amido complexes are bent and others are planar with the bent structures having dihedral angles ranging from 32−45°. The two halves of the core appear to be chemically, though not crystallographically, equivalent, and the two Pd−O and Pd−N distances are indistinguishable and are 2.14 and 2.08 Å, respectively. Despite the larger size of nitrogen and the presence of an N-bound alkyl group, the Pd−N distances are shorter than the Pd−O distances. As demonstrated below, the shorter distance is not a result of a stronger Pd−N bond.[45]

Table 2. Selected Intramolecular Distances for $\{Pd_2(PPh_3)_2Ph_2(\mu\text{-OH})(\mu\text{-NH-}t\text{-Bu})\}$(3a)[a]

Pd1−Pd2	2.905(1)	Pd2−P2	2.251(2)
Pd1−P1	2.253(2)	Pd2−O1	2.140(4)
Pd1−O1	2.142(5)	Pd2−N1	2.086(6)
Pd1−N1	2.083(5)	Pd2−C25	2.015(7)
Pd1−C1	1.989(7)	N1−C49	1.49(1)
		O1−H53	0.798

[a] Distances are in angstroms. Estimated standard deviations in the least significant figure are given in parentheses.

Table 3. Selected Intramolecular Angles for $\{Pd_2(PPh_3)_2Ph_2(\mu\text{-OH})(\mu\text{-NH-}t\text{-Bu})\}$(3a)[a]

Pd2−Pd1−P1	130.17(6)	P2−Pd2−O1	99.3(1)
Pd2−Pd1−O1	47.3(1)	P2−Pd2−N1	178.7(2)
Pd2−Pd1−N1	45.9(2)	P2−Pd2−C25	91.5(2)
Pd2−Pd1−C1	122.9(2)	O1−Pd2−N1	79.3(2)
P1−Pd1−O1	97.6(1)	O1−Pd2−C25	169.1(2)
P1−Pd1−N1	176.1(2)	N1−Pd2−C25	89.8(3)
P1−Pd1−C1	89.7(2)	Pd1−O1−Pd2	85.4(2)
O1−Pd1−N1	79.4(2)	Pd1−N1−Pd2	88.3(2)
O1−Pd1−C1	170.2(2)	Pd1−N1−C49	120.5(4)
N1−Pd1−C1	93.1(2)	Pd2−N1−C49	118.7(4)
Pd1−Pd2−P2	133.07(6)	Pd1−O1−H53	120.41
Pd1−Pd2−O1	47.3(1)	Pd2−O1−H53	126.05
Pd1−Pd2−N1	45.8(1)	Pd1−N1−H41	109.17
Pd1−Pd2−C25	124.0(2)	Pd2−N1−H41	109.17
		C49−N1−H41	109.17

[a] Angles are in degrees. Estimated standard deviations in the least significant figure are given in parentheses.

N−H Bond-Forming Reactions. The proton exchange reactions of **1** with primary amines to generate palladium amido complexes and H_2O are reversible. Heating a THF solution of the alkyl- or arylamido complexes **2a,b** and **3a**−**c** with 100 equiv of H_2O at 70 °C for 1.5 h gave complete consumption of the amido complex and regenerated **1** as the only species observed by ^{31}P NMR spectroscopy. The proton exchange reaction with thiols, however, was not reversible. Heating a THF solution of **5** with an excess of water at 70 °C for several hours led to complete decomposition of **5** with no formation of **1**. GC/MS indicated the formation of a variety of sulfur-containing organic compounds.

Thermodynamic Analysis of the NH Bond Cleavage. As discussed above, **1** reacts reversibly with primary amines to give palladium amides and water. This reversibility allowed for measurement of the equilibrium constants, K_{eq}, of these proton exchange reactions and calculation of ΔH and ΔS for the reactions.[46] The rapid reaction of **1** with aniline to generate **2a** and H_2O (eq 1) was used to determine the temperature

(42) Louie, J.; Hartwig, J. F. *J. Am. Chem. Soc.* **1995**, *117*, 11598.
(43) X-ray data for **3a** was previously submitted as Supporting Information, see: Driver, M. S.; Hartwig, J. F. *J. Am. Chem. Soc.* **1996**, *118*, 4206−4207.
(44) For a well-characterized example and related references, see: Ruiz, J.; Martinez, M. T.; Vicente, C.; Garcia, G.; Lopez, G.; Chaloner, P.; Hitchcock, P. B. *Organometallics* **1993**, *12*, 4321.
(45) For a recent discussion of bond lengths and strengths, see: Ernst, R. D.; Freeman, J. W.; Stahl, L.; Wilson, D. R.; Arif, A. M.; Nuber, B.; Ziegler, M. L. *J. Am. Chem. Soc.* **1995**, *117*, 5075.

dependence of K_{eq}. Data were obtained by monitoring

$$\mathbf{1} + H_2NPh \rightleftharpoons \mathbf{2a} + H_2O$$

$$\Delta H = -3.6 \text{ kcal/mol } \Delta S = 1.2 \text{ eu} \qquad (1)$$

the relative concentrations of **1** and **2a** in a THF solution by ^{31}P NMR spectroscopy between −20 and 40 °C. Below −20 °C, material precipitated from solution. The graph of $\ln(K_{eq})$ vs $-1/T$ (Figure S1)[47] was linear and resulted in a $\Delta H°$ of -3.6 ± 0.4 kcal·mol^{-1} and $\Delta S°$ of 1.2 ± 0.9 eu, indicating a small entropic contribution to $\Delta G°$. The equilibrium constant for the reaction of **1** with *sec*-butylamine (eq 2) was measured in a similar fashion and was found to be 12, which corresponds to $\Delta G_{298}°$ of −1.5 kcal·mol^{-1}.

$$\mathbf{1} + H_2N\text{-}sec\text{-}Bu \overset{K_{eq} = 12}{\rightleftharpoons} \mathbf{3b} + H_2O$$

$$\Delta G = -1.5 \text{ kcal/mol} \qquad (2)$$

Mechanism of NH Bond Cleavage by 1. The cleavage of the NH bond of an amine to generate a reactive metal−amido complex is an important step for observing transition metal reaction chemistry with amine substrates. The proposed catalytic cycle for the addition of aniline across an olefin involves activation of an NH bond to generate a reactive Ir amido complex.[32] More recently, it has been proposed that palladium alkoxide complexes may activate the NH bond of amines to generate the reactive palladium amido complexes involved in the catalytic amination of aryl halides.[48] A better understanding of how the NH bond of an amine is activated to generate reactive amido intermediates will aid in the development of improved processes for the utilization of amine substrates.

We began our investigation of the mechanism of the NH activation reaction by studying the reaction of **1** with *sec*-butylamine. Kinetic data for the reaction of **1** with *sec*-butylamine were obtained by monitoring the decay of the rapidly equilibrating isomers of **1** by ^1H NMR spectroscopy in THF-d_8 solvent at 25 °C. The reactions were conducted under conditions that were pseudo-first-order in [**1**]. Plots of ln[**1**] vs time (Figure S2) were linear over 3 half-lives, and reaction rates were independent of $[\mathbf{1}]_0$, indicating a first-order dependence on [**1**]. A graph of $\ln(k_{obs})$ vs ln[*sec*-butylamine] (Figure S3) was linear with a slope of 2.0 ± 0.1, demonstrating a *second*-order dependence on [*sec*-butylamine]. This reaction order is surprising considering that only one amido ligand is incorporated into the product **3b**. Reaction rates were independent of added PPh_3 (130−390 mM). Another set of reactions were conducted with added H_2O. The graph of $1/k_{obs}$ vs $[H_2O]$ in Figure 2 was linear with a positive slope and a non-zero *y*-intercept. These data indicate that the reaction is inhibited by added H_2O but that the reaction order in water is not simply inverse first order. Finally, reactions using deuterium-labeled **1**-(μ-OD)$_2$ with D_2N-*sec*-butyl revealed an inverse isotope effect, $k_H/k_D = 0.7 \pm 0.1$.

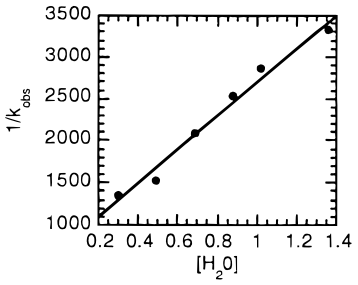

Figure 2. Plot of $1/k_{obs}$ vs $[H_2O]$. $R = 0.99$.

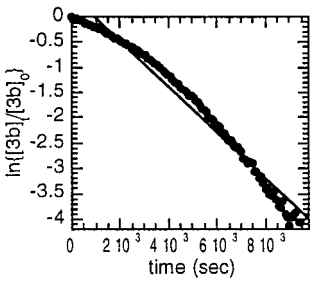

Figure 3. Plot of $\ln\{[\mathbf{3b}]_t/[\mathbf{3b}]_0\}$ vs time for the reaction of **3b** with H_2O in the absence of H_2N-*sec*-Bu. The graph deviates from linearity because k_{obs} of eq 8 changes as a result of the increasing [H_2N-*sec*-Bu] over the course of the reaction.

To gain a better understanding of the chemistry of amines and of the amido complexes, we studied the reverse of the N−H bond cleavage, reaction of **3b** with H_2O to form **1** and free amine. Study of the reaction of **3b** with H_2O will reveal information about steps of the N−H bond cleavage process that occur after the rate-determining step. Kinetic data for the reaction of **3b** with H_2O were again obtained by ^1H NMR spectroscopy in THF-d_8 solvent, this time at 70 °C and under conditions that are pseudo-first-order in **3b**. Plots of ln[**3b**] vs time (Figure S4) were linear over 3 half-lives, indicating first-order behavior in [**3b**]. In contrast to the N−H bond cleavage process, the reaction rates were independent of $[D_2O]$, even though the transformation involved reaction of **3b** with D_2O. Monitoring the reaction at varied [*sec*-butylamine] and graphing $\ln(k_{obs})$ vs ln[*sec*-butylamine] (Figure S5) resulted in a line with a slope of 1.0 ± 0.1, indicating that the reaction is first order in [*sec*-butylamine]. Since the reaction is first order in amine while amine is a product of the reaction, this reaction of **3b** with water is autocatalytic. Indeed, reactions of **3b** with water in the absence of added amine showed autocatalytic behavior. A plot of ln[**3b**] vs time (Figure 3) deviates from linearity as a result of the changing concentration of amine product. We have not been able to ascertain the initiation process that generates amine.

Discussion

Reversibility of the Proton Transfer Reactions of 1 with Amines. The reactivity of **1** with free amines to produce palladium amido complexes and water stands in marked contrast to the reactivity predicted by pK_a values and the reactivity of main group and early metal amides with water. In organic solvents, the pK_a[49] of H_2O was measured to be approximately 31 while that

(46) The concentrations of water and amine were calculated based on their known starting concentrations and the stoichiometry of the reaction depicted in eq 1.

(47) Figures S1−S5 are provided as Supporting Information.

(48) Mann, G.; Hartwig, J. F. *J. Am. Chem. Soc.* **1996**, *118*, 13109−13110.

(49) Bordwell, F. G. *Acc. Chem. Res.* **1988**, *21*, 456−463.

of ammonia was estimated to be 41, indicating H_2O is much more acidic than ammonia and presumably alkylamines. This suggests that H_2O should react with the amido anion to give amine and hydroxide. In the reactions of main group and early transition metal amides with H_2O, this is indeed the case. Alkali-metal amides react violently with H_2O to form the corresponding hydroxide and free amine. Also, the early metal amido complex $Cp^*_2Hf(NH_2)H$ reacts rapidly with H_2O to give $Cp^*_2Hf(OH)H$ and NH_3.[2]

However, late transition metal organometallic complexes are often more stable toward water; similarly, late metal amido complexes appear to be more stable toward water than early metal amides. The addition of diarylamines to $Cp^*(PMe_3)_2Ru(OH)$ established an equilibrium that favored the hydroxide complex,[50] while addition of diarylamines to (DPPE)Pt(Me)(OH) favored formation of the amido complexes, as observed for the reaction of the alkylamines with the palladium hydroxo dimer (*vide supra*).[44] Apparently, metal amido complexes become increasingly more stable toward reaction with H_2O as one moves to the right in the transition metal series.

Thermodynamic Analysis of Proton Transfer Reactions of 1 with Primary Amines. The reversibility of the reactions of **1** with primary amines allowed for the measurement of the thermodynamic parameters for the proton transfer reactions and the relative Pd−(μ-OH)−Pd and Pd−(μ-NHR)−Pd bond strengths. The entropic term of the proton exchange reaction was small, $\Delta S° = 1.2$ eu, as would be expected considering the equal numbers of molecules on either side of eq 1. Using ΔH_{rxn} of 3.6 kcal·mol^{-1} along with the known 119 kcal·mol^{-1} O−H bond strength of water and the 88 kcal·mol^{-1} N−H bond strength of aniline,[51] we calculated that the bridging Pd−(μ-OH)−Pd interaction is stronger than the bridging Pd−(μ-NHAr)−Pd interaction by approximately 27 kcal·mol^{-1}.

The reaction of **1** with *sec*-butylamine was also reversible, and the K_{eq} was measured to be 12, corresponding to a $\Delta G_{298}° = -1.5$ kcal·mol^{-1}. Since ΔS for the similar reaction involving aniline was small, one can assume that $\Delta G_{298}° \cong \Delta H°$ in this case as well. From the ΔH_{rxn} of 1.5 kcal·mol^{-1}, the 119 kcal·mol^{-1} O-H bond strength of water, and the presumably similar N−H bond strength of *sec*-butylamine to the 100 kcal·mol^{-1} N−H bond strength in H_2NMe,[51] we concluded that the bridging Pd−(μ-OH)−Pd interaction is stronger that the bridging Pd−(μ-NHR)−Pd interaction by roughly 17 kcal·mol^{-1}.

The relative M−X bond strengths for various ligands have previously been measured for the systems $Cp^*(PMe_3)_3Ru-X$ and (DPPE)MePt−X,[50] $Cp^*_2(OCMe_3)Th-X$,[52] and $Cp^*(PMe_3)(H)Ir-X$[53] with a detailed discussion and comparison presented by Bryndza and Bercaw.[50] In these studies, a linear correlation between the relative L_nM-X bond strengths and H−X bond strengths was found where X was a terminal, covalent ligand. This linear relationship appeared to be a general trend that

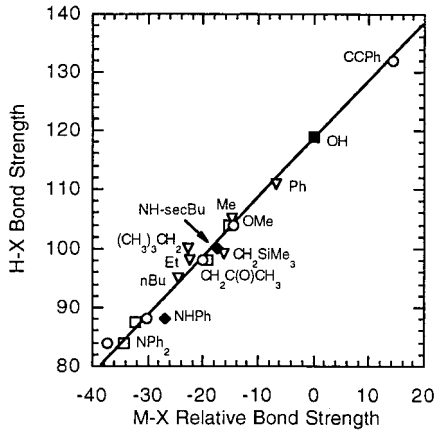

Figure 4. H−X vs relative L_nM-X bond strengths in kcal·mol^{-1}. Amido ligand bond strengths (♦) calculated for **2a** and **3b** superimposed on values for (DPPE)Pt(Me)X (■), $Cp^*(PMe_3)_2Ru-X$ (○), and $Cp^*_2(OCMe_3)ThX$ (▽) from refs 50 and 52 with L_nM-OH bond strength arbitrarily assigned to 0 kcal·mol^{-1}.

was independent of the identity of the metal fragment (Figure 4), in the absence of M−X multiple bonding.[52] Many amido and alkoxo ligands bridge between two metal centers. Thus, it is important to understand how bridging interactions affect the relative bond strengths.

Perhaps surprisingly, one can see that the bridging amido bond strengths lie on the linear correlation between L_nM-X and H−X bond strengths established from the Bryndza and Bercaw study and Marks study (Figure 4). For this analysis, the bridging hydroxide interaction was assigned as 0 in our case, and the hydroxide bond strength was designated 0 in the Bryndza and Marks studies. One might expect the more basic N electron pair to be a stronger donor to the Pd center than the O lone pair electrons, making the relative bond strengths for a combination of the two bridging interactions substantially different than the relative strengths for the terminal ligands. The close correlation of bridging amido bond strengths to the terminal values demonstrates otherwise. To the extent that the bonds of the bridging group can be dissected into one covalent and one dative bond, the dative interaction of the amido group is either not substantially stronger than that of the hydroxo group or the stronger dative interaction is accompanied by weakening of the covalent interaction.

Mechanism of Proton Exchange Reaction of 1 with *sec*-Butylamine. Potential mechanisms for the reaction of **1** with *sec*-butylamine are shown in Schemes 3 and 4. Pathway A consists of initial reversible dimer cleavage to form two three-coordinate species, followed by coordination of amine. After coordination of amine, reversible proton transfer occurs to form the amido ligand and water, which dissociates to form a three-coordinate amido species. This amido species then associates with a three-coordinate hydroxo complex to give the product **3b**. There is a significant problem with this mechanism. We have shown previously that three-coordinate PPh_3-ligated palladium alkyl amido complexes undergo reductive elimination faster than dimerization.[54] Although the dimerization of a three-coordinate amido complex is slightly different from trapping by the three-coordinate hydroxo complex, one would expect to see some reductive elimination products; no *N*-alkyl

(50) Bryndza, H. E.; Fong, L. K.; Paciello, R. A.; Tam, W.; Bercaw, J. E. *J. Am. Chem. Soc.* **1987**, *109*, 1444.
(51) McMillen, D. F.; Golden, D. M. *Ann. Rev. Phys. Chem.* **1982**, *33*, 493−532.
(52) Bruno, J. W.; Marks, T. J.; Morss, L. R. *J. Am. Chem. Soc.* **1983**, *105*, 6824−6832.
(53) Buchanan, J. M.; Stryker, J. M.; Bergman, R. G. *J. Am. Chem. Soc.* **1986**, *108*, 1537.

Scheme 3

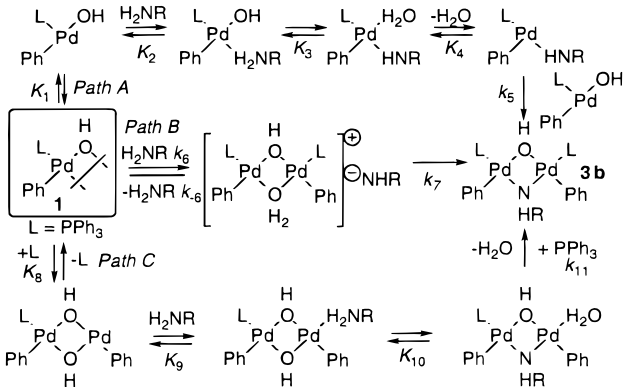

arylamine products were observed. Pathway A would follow the rate expression in eq 3, which predicts a first-order dependence on **1**, a first-order dependence on [amine], and an inverse-first-order dependence on [H_2O]. In contrast to this prediction, the N−H bond

$$\frac{-\mathrm{d}[\mathbf{1}]}{\mathrm{d}t} = k_{\mathrm{obs}}[\mathbf{1}] \text{ where}$$

$$k_{\mathrm{obs}} = \frac{K_1K_2K_3K_4k_5[\mathrm{H_2N\text{-}}\textit{sec}\text{-Bu}]}{[\mathrm{H_2O}]} \qquad (3)$$

cleavage process showed a second-order dependence on [amine], rigorously ruling out pathway A.

Pathway B depicts direct deprotonation of the amine substrate to form a coordinated H_2O. The water ligand would then be displaced by the amide anion to form the product **3b**. This pathway would give rise to the rate expression in eq 4, which includes a first-order dependence on **1**, a first-order dependence on [amine], and a zero-order dependence on [H_2O]. This mechanism is

$$\frac{-\mathrm{d}[\mathbf{1}]}{\mathrm{d}t} = k_{\mathrm{obs}}[\mathbf{1}] \text{ where}$$

$$k_{\mathrm{obs}} = \frac{k_6k_7[\mathrm{H_2N\text{-}}\textit{sec}\text{-Bu}]}{k_{-6} + k_7} \qquad (4)$$

ruled out by the observed second-order dependence on [amine] and the inhibition of the reaction by added water.

Pathway C involves reversible phosphine dissociation from **1** to create a position for amine coordination. After amine coordination, proton transfer would occur to form the amido ligand and water. In the final step, phosphine would reassociate with the Pd complex to displace the water and form **3b**. This mechanism would follow the rate expression in eq 5, which predicts a first-order dependence on [**1**], a first-order dependence on [amine], and a zero-order dependence on [H_2O]. There is no

$$\frac{-\mathrm{d}[\mathbf{1}]}{\mathrm{d}t} = k_{\mathrm{obs}}[\mathbf{1}] \text{ where}$$

$$k_{\mathrm{obs}} = K_8K_9K_{10}k_{11}[\mathrm{H_2N\text{-}}\textit{sec}\text{-Bu}] \qquad (5)$$

phosphine dependence as a result of both dissociation and association occuring before or as part of the rate-determining step. Most important, the predicted order in [amine] and [H_2O] are different from the ones observed, ruling out the dissociative mechanism of pathway C.

Paths D depict two kinetically related mechanisms in which 2 equiv of amine are involved in the N−H cleavage process. In the top mechanism of path D, 2 equiv of amine react with dimeric **1** by an associative process to generate 2 equiv of a monomer with a terminal hydroxo ligand and a coordinated amine on the same complex. In the bottom mechanism, 1 equiv of amine is used to generate a terminal hydroxo ligand in a bimetallic intermediate. The subsequent step in these mechanisms would involve reversible proton transfer between one of the amines, either coordinated or uncoordinated, and one of the hydroxo ligands to form coordinated or free water and an amido ligand. In the case of the top path D the amido aquo intermediate would combine with one of the amino hydroxo intermediates to give a dinuclear μ-OH complex, while in the case of the bimetallic mechanism, the same dinuclear μ-OH intermediate would be formed by exchange of the hydroxo ligand with amine. This exchange may or may not involve coordination of amine. In the final step, the amido ligand replaces the coordinated amine to form **3b**. Both mechanisms in path D would show a first-order dependence on [**1**], a second-order dependence on [amine], and an order in [H_2O] that depends on the water concentration. The rate expressions for paths D are given in eq 6; the order in [H_2O] for this mechanism is best revealed by inverting eq 6 to generate eq 7. Equation 7 shows that a plot of $1/k_{\mathrm{obs}}$ vs [H_2O]

$$\frac{-\mathrm{d}[\mathbf{1}]}{\mathrm{d}t} = k_{\mathrm{obs}}[\mathbf{1}] \text{ where}$$

$$k_{\mathrm{obs}} = \frac{K_{12}K_{13}k_{14}k_{15}[\mathrm{H_2N\text{-}}\textit{sec}\text{-Bu}]^2}{k_{-14}[\mathrm{H_2O}] + k_{15}} \text{ or } \frac{K_{16}k_{17}k_{15}[\mathrm{H_2N\text{-}}\textit{sec}\text{-Bu}]^2}{k_{-17}[\mathrm{H_2O}] + k_{15}} \qquad (6)$$

$$\frac{1}{k_{\mathrm{obs}}} = \frac{k_{-14}[\mathrm{H_2O}]}{K_{12}K_{13}k_{14}k_{15}[\mathrm{H_2N\text{-}}\textit{sec}\text{-Bu}]^2} + \frac{1}{K_{12}K_{13}k_{14}[\mathrm{H_2N\text{-}}\textit{sec}\text{-Bu}]^2} \qquad (7)$$

$$\text{or } \frac{k_{-17}[\mathrm{H_2O}]}{K_{16}K_{17}k_{15}[\mathrm{H_2N\text{-}}\textit{sec}\text{-Bu}]^2} + \frac{1}{K_{16}k_{17}[\mathrm{H_2N\text{-}}\textit{sec}\text{-Bu}]^2}$$

will be linear with a non-zero *y*-intercept. This behavior is exactly what was observed in Figure 2. The complex order in [H_2O] shows that the mechanism involves reversible formation of water followed by replacement of the amine ligand by the amide to form **3b**.

In addition, the reversible proton transfer step will provide a kinetic isotope effect that originates from the proton transfer equilibrium. The value of K_H/K_D for the proton transfer and, therefore, the k_H/k_D for the overall reaction is likely to be <1 as a result of the higher ν_{OH} than ν_{NH}. An inverse isotope effect, $k_H/k_D = 0.7$, was observed for the reaction of **1**-(μ-OD)$_2$ with D_2N-*sec*-Bu. *All of our kinetic data are consistent with the proton transfer reaction of* ***1*** *with sec-butylamine proceeding via*

(54) Driver, M. S.; Hartwig, J. F. *J. Am. Chem. Soc.* **1995**, *117*, 4708−4709.

Scheme 4. Path D

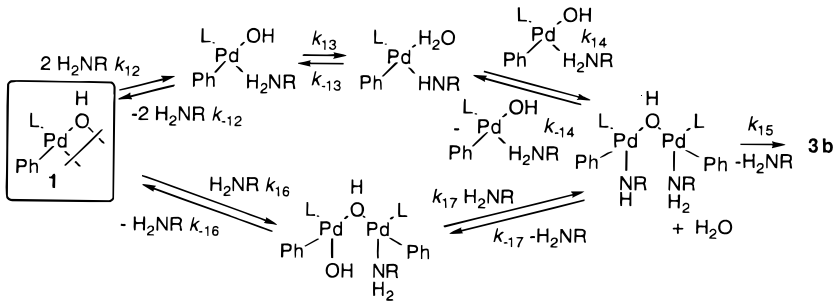

amine-facilitated generation of a terminal hydroxo ligand by one of the two kinetically indistinguishable mechanisms in path D.

The principle of microscopic reversibility states that a reaction must follow the same mechanism in both the forward and reverse directions. Since the reaction of **1** with *sec*-butylamine to produce **3b** and H_2O is reversible, we studied the reaction in the reverse direction in order to add further support for our mechanistic conclusions, since the involvement of two amines in the N−H cleavage process is counterintuitive. For the reverse reaction, addition of water to **3b**, the mechanisms shown in path D of Scheme 4 would result in the rate expressions shown in eq 8, assuming that k_{-14} or k_{-17} is irreversible. In order for the reaction to proceed, a

$$\frac{-\mathrm{d}[\mathbf{3b}]}{\mathrm{d}t} = k_{\mathrm{obs}}[\mathbf{3b}] \text{ where}$$

$$k_{\mathrm{obs}} = \frac{k_{-14}k_{-15}[\mathrm{H_2N\text{-}}sec\text{-}\mathrm{Bu}][\mathrm{H_2O}]}{k_{-14}[\mathrm{H_2O}] + k_{15}} \text{ or } \frac{k_{-17}k_{-15}[\mathrm{H_2N\text{-}}sec\text{-}\mathrm{Bu}][\mathrm{H_2O}]}{k_{-17}[\mathrm{H_2O}] + k_{15}} \quad (8)$$

high $[H_2O]$ is necessary. Under these conditions, the $k_{-14}[H_2O]$ or $k_{-17}[H_2O]$ term in the denominator is much larger than k_{15} and the rate expression simplifies to the one shown in eq 9. This expression predicts a first-order

$$\frac{-\mathrm{d}[\mathbf{3b}]}{\mathrm{d}t} = k_{\mathrm{obs}}[\mathbf{3b}] \text{ where}$$

$$k_{\mathrm{obs}} = k_{-15}[\mathrm{H_2N\text{-}}sec\text{-}\mathrm{Bu}] \quad (9)$$

dependence on [**3b**], a first-order dependence on [amine], and no dependence on $[H_2O]$. Indeed, our kinetic data showed these reaction orders. Since the rate expression includes a first-order term in the product amine, the amine produced over the course of the reaction will catalyze the addition of water to **3b**. In other words, the involvement of the extra amine in the forward reaction should give rise to autocatalytic behavior in amine for the reverse reaction, and this autocatalytic behavior was observed. In this case, the extra amine appears to be used to generate a terminal amido or hydroxo ligand that is more basic than the bridging ligand and can deprotonate the water or amine substrate.

Conclusions

The N−H bond cleavage chemistry of amines with late transition metals is not well-studied. Although the oxidative addition of acidic N−H bonds or those activated by chelation has been observed a number of times,[32,55−60] the oxidative addition of the less acidic NH bonds of alkylamines and ammonia has only been observed in a few cases and most of these are with early metals.[2] The reaction of ammonia with $(PEt_3)_2Ir(C_2H_4)_2$-Cl to give a dimeric iridium amido complex is the only report of the oxidative addition of ammonia to a late transition metal system.[10] The only reports of the oxidative addition of alkylamines have occurred with Os clusters.[7,8] Reactions of late transition metal complexes with the NH bonds of activated amines has also occurred by proton exchanges,[44,50] but such σ-bonded ligand exchanges with alkylamines are even more unusual than oxidative addition of alkylamine N−H bonds. Presumably, the absence of proton transfer chemistry with alkylamines is due to their weak Brønsted acidity and strong Lewis basicity.

The σ-bonded ligand exchange is formally acid−base chemistry, analogous to the deprotonation of an amine by an alkali metal reagent. However, two features of the palladium chemistry are remarkable. First, the thermodynamics of the acid−base chemistry are the opposite of what would be expected from pK_a data. Streitwieser has shown that the ion-pair acidities of metal amides are highly dependent on the identity of the metal.[61] For example, the pK's of the lithium and cesium ion pairs of diphenylamide differ by 5 pK units at 19.05 and 24.20, respectively. Some of this difference can be explained by the aggregation number, but the type of ion pair and the strength of the metal amide interaction are also important. In the N−H bond cleavage chemistry described in this work, the countercation is the palladium fragment and the amide and hydroxide are transition metal complexes rather than alkali metal complexes. By the definition of ion-pair acidities, the amine is actually more acidic than water in these organic solvents when a palladium fragment serves as the counterion. Second, the acid−base chemistry occurs with mild reagents. Both the palladium hydroxo complex and amide products are air stable. This property stands in contrast to the typical reagents that react with amine N−H bonds such as organolithium

(55) Samat, A.; Sala-Pala, J.; Guglielmetti, R.; Guerchais, J. *Nouv. J. Chem.* **1978**, *2*, 13−14.
(56) Ladipo, F. T.; Merola, J. S. *Inorg. Chem.* **1990**, *29*, 4172−4173.
(57) Hsu, G. C.; Kosar, W. P.; Jones, W. D. *Organometallics* **1994**, *13*, 385−396.
(58) Jones, W. D.; Dong, L.; Myers, A. W. *Organometallics* **1995**, *14*, 855−861.
(59) Fornies, J.; Green, M.; Spencer, J. L.; Stone, F. G. *J. Chem. Soc., Dalton Trans.* **1977**, 1006−1009.
(60) Park, S.; Hedden, D.; Roundhill, D. M. *Organometallics* **1986**, *5*, 2151.
(61) Krom, J. A.; Petty, J. T.; Streitwieser, A. *J. Am. Chem. Soc.* **1993**, *115*, 8024−8030.

reagents or alkali metals, all of which are highly air sensitive and which are typically incapable of being used as catalysts. Thus, the palladium chemistry offers a pathway for formation of a metal amido species that is mild and that offers a means for catalytic modification of the amine substrate.

This result is important for the further development of transition metal catalyzed chemistry of amines. For example, our laboratory and Buchwald's have developed a catalytic process for the amination of aryl halides in the presence of alkoxide base.[33,34] Our work on proton exchange reactions presented here along with studies conducted on isolated palladium alkoxide complexes[48] have shown that the alkoxide complexes (DPPF)Pd(Ar)-(O-*t*-Bu) undergo proton transfer reactions with free amines to generate reactive palladium amido complexes, which then reductively eliminate coupled amine product. These results suggest that alkoxide complexes may be intermediates in the conversion of aryl halide complexes to arylamido complexes in the amination chemsitry and, more generally, that alkoxide complexes may be used for the production of amido complexes by N−H activation.

Experimental Section

General Methods. Unless otherwise noted, all reactions and manipulations were performed in an inert atmosphere glovebox or by using standard Schlenk techniques. Benzene, toluene, THF, ether, and pentane solvents were distilled from sodium/benzophenone prior to use. Amines were distilled from CaH_2, and triphenylphosphine was sublimed prior to use in kinetic studies. Both H_2O and D_2O were degassed with N_2(g) before use in kinetic studies. All other chemicals were used as received from commercial suppliers.

Preparation of [(PPh$_3$)(C$_6$H$_5$)Pd(μ-OH)]$_2$ (1). Into a 20 mL vial was weighed 150 mg (0.180 mmol) of *trans*-$(PPh_3)_2$-Pd(C_6H_5)(I).[62] The solid material was dissolved in 12 mL of THF with stirring. CsOH (400 mg, 2.7 mmol) was added to the vial as a solid. The reaction was stirred at room temperature for 2 h. A $^{31}P\{^1H\}$ NMR spectrum of the reaction mixture indicated complete consumption of the starting material. The reaction mixture was filtered through a medium-fritted funnel containing Celite, and the resulting clear solution was concentrated under vacuum. Pentane was added to precipitate the product. The product was collected on a medium-fritted funnel to give 137 mg (83%) of white solid. The $^{31}P\{^1H\}$ and ^1H NMR spectra matched those previously published.[40]

Preparation of (PPh$_3$)(C$_6$H$_5$)Pd(μ-OH)(μ-NHC$_6$H$_5$)Pd-(C$_6$H$_5$)(PPh$_3$) (2a). Into a vial was weighed 128 mg (0.138 mmol) of **1**. The solid material was dissolved in 8 mL of THF, and 63 μL (0.693 mmol) of aniline was added to the reaction solution. The reaction was stirred at room temperature for 30 min. A $^{31}P\{^1H\}$ NMR spectrum of the reaction mixture indicated complete consumption of the starting material and the formation of **2a** as a mixture of *syn*- and *anti*-isomers. The reaction solution was filtered through Celite, concentrated, and layered with Et_2O. The THF/Et_2O solution was cooled at −20 °C to yield 121 mg (88%) of amber crystalline **2a** as predominately (>90%) the *syn*-isomer. ^1H NMR: (C_6D_6, *syn*-isomer) δ −3.40 (s, 1H), 2.75 (t, J = 4.2 Hz, 1H), 6.63−6.78 (m, 5H), 6.81−6.89 (m, 20H), 7.19−7.22 (m, 6H), 7.44−7.50 (m, 12H), 7.62 (d, J = 7.8 Hz, 2H); (C_6D_6, *anti*-isomer) δ −1.53 (d, J = 3.4 Hz, 1H), 1.55 (d, J = 4.8 Hz, 1H). $^{31}P\{^1H\}$ NMR (THF): δ 34.1, 31.5 (*anti*-isomer), 29.8 (*syn*-isomer). IR (cm^{-1}, KBr): 3603 (m, ν_{OH}), 3322 (w, ν_{NH} *syn*-isomer), 3308 (w, ν_{NH} *anti*-isomer). Anal. Calcd for $C_{54}H_{47}NOP_2Pd_2\cdot Et_2O$ (confirmed by integrated ^1H NMR spectra): C, 64.81; H, 5.35; N, 1.30. Found: C, 64.52; H, 5.66; N, 1.30.

Preparation of *syn*-(PPh$_3$)(C$_6$H$_5$)Pd(μ-OH)(μ-NH-2,6-(CH$_3$)$_2$C$_6$H$_3$)Pd(C$_6$H$_5$)(PPh$_3$) (2b). Into a screw-capped test tube was weighed 186 mg (0.201 mmol) of **1**. The solid material was dissolved in 8 mL of THF, and H_2N-2,6-$(CH_3)_2C_6H_3$ (0.25 mL, 2.01 mmol) was added to the test tube. The test tube was sealed, and the reaction was stirred at 70 °C for 1 h. A $^{31}P\{^1H\}$ NMR spectrum of the reaction mixture indicated complete consumption of the starting material. The reaction mixture was filtered through Celite, concentrated and layered with Et_2O. The THF/Et_2O solution was cooled at −35 °C to yield 120 mg (58%) of white crystalline material. ^1H NMR (C_6D_6): δ −4.11 (s, 1H), 1.12 (s, 3H), 3.29 (t, J = 5.0 Hz, 1H), 4.43 (s, 3H), 6.51−6.61 (m, 6H), 6.80 (t, J = 7.0 Hz, 2H), 6.92−7.09 (m, 21H), 7.42 (d, J = 6.0 Hz, 2H), 7.50−7.61 (m, 12H). $^{31}P\{^1H\}$ NMR (THF): δ 27.5. $^{13}C\{^1H\}$ NMR (C_6D_6): δ 17.9 (s), 24.6 (s), 118.9 (s), 122.2 (s), 126.2 (s), 127.1 (s), 128.3 (d, J = 10.3 Hz), 128.9 (s), 129.2 (s), 130.0 (s), 131.4 (s), 131.8 (d, J = 43.1 Hz), 134.5 (d, J = 11.9 Hz), 136.3 (d, J = 3.7 Hz), 149.9 (d, J = 7.3 Hz), 151.3 (t, J = 2.8 Hz). IR (cm^{-1}, KBr): 3622 (w, ν_{OH}), 3326 (w, ν_{NH}). Anal. Calcd for $C_{56}H_{51}NOP_2Pd_2$: C, 65.38; H, 5.00; N, 1.36. Found: C, 65.03; H, 5.41; N, 1.20.

Preparation of *syn*-(PPh$_3$)(C$_6$H$_5$)Pd(μ-OH)(μ-NH-*t*-Bu)-Pd(C$_6$H$_5$)(PPh$_3$) (3a). Into a screw-capped test tube was weighed 103 mg (0.111 mmol) of **1**. H_2N-*t*-Bu (8 mL) was added to the test tube. The test tube was sealed and heated at 70 °C with stirring for 1 h. The reaction mixture became homogeneous. A $^{31}P\{^1H\}$ NMR spectrum of the reaction mixture indicated complete consumption of the starting material. The reaction mixture was filtered through Celite and concentrated. The THF solution was layered with Et_2O and cooled at −35 °C to yield 68.5 mg (63%) of white crystalline material. ^1H NMR (C_6D_6): δ −3.10 (s, 1H), 1.54 (t, 6.0 Hz, 1H), 1.64 (s, 9H), 6.83−6.94 (m, 24H), 7.57−7.66 (m, 16H). $^{31}P\{^1H\}$ NMR (THF): δ 26.2. $^{13}C\{^1H\}$ NMR (C_6D_6) δ: 36.7 (s), 59.1 (s), 122.3 (s), 127.1 (s), 128.3 (apparent t, J = 5.0 Hz), 129.9 (s), 132.2 (d, J = 42.2 Hz), 134.7 (apparent t, J = 6.2 Hz), 138.5 (s), 150.7 (d, J = 10.4 Hz). IR (cm^{-1}, KBr): 3619 (w, ν_{OH}). Anal. Calcd for $C_{52}H_{51}NOP_2Pd_2\cdot THF\cdot 0.5Et_2O$ (confirmed by integrated ^1H NMR spectra): C, 63.92; H, 5.92; N, 1.29. Found: C, 63.84; H, 5.96; N, 1.39.

Preparation of *syn*-(PPh$_3$)(C$_6$H$_5$)Pd(μ-OH)(μ-NH-*sec*-Bu)Pd(C$_6$H$_5$)(PPh$_3$) (3b). Into a screw-capped test tube was weighed 102 mg (0.110 mmol) of **1**. The solid material was dissolved in 8 mL of THF, and H_2N-*sec*-Bu (55 μL, 0.550 mmol) was added to the test tube. The test tube was sealed, and the reaction was stirred at room temperature for 5 h. A $^{31}P\{^1H\}$ NMR spectrum of the reaction mixture indicated complete consumption of the starting material. The reaction mixture was filtered through Celite. The THF solution was concentrated and layered with Et_2O. The THF/Et_2O solution was cooled at −35 °C to yield 77.5 mg (72%) of white crystalline material. ^1H NMR (C_6D_6): δ −3.25 (s, 1H), 0.63 (t, J = 7.4 Hz, 3H), 1.43 (m, 1H), 1.57 (apparent hept, J = 6.9 Hz, 1H), 1.78 (d, J = 6.3 Hz, 3H), 1.96 (apparent hept, J = 6.6 Hz, 1H), 3.68 (m, 1H), 6.78−6.93 (m, 24H), 7.54−7.62 (m, 16H). $^{31}P\{^1H\}$ NMR (THF): δ 27.3 (s), 27.1 (s). $^{13}C\{^1H\}$ NMR (C_6D_6): δ 11.0 (s), 26.2 (s), 35.1 (s), 58.2 (s), 122.0 (s), 122.0 (s), 126.8 (s), 126.9 (s), 128.1 (d, J = 12.1 Hz), 128.1 (d, J = 12.1 Hz), 129.6 (s), 129.62 (s), 132.0 (d, J = 41.8 Hz), 132.2 (d, J = 42.1 Hz), 134.3 (d, J = 11.7 Hz), 134.3 (d, J = 11.7 Hz), 137.3 (d, J = 2.4 Hz), 137.7 (d, J = 2.8 Hz), 150.2 (d, J = 9.7 Hz), 151.5 (d, J = 10.1 Hz). IR (cm^{-1}, KBr): 3611 (w, ν_{OH}), 3301 (w, ν_{NH}). Anal. Calcd for $C_{56}H_{51}NOP_2Pd_2$: C, 63.68; H, 5.24; N, 1.43. Found: C, 63.50; H, 5.32; N, 1.36.

Preparation of *anti*-[(PPh$_3$)(C$_6$H$_5$)Pd(μ-NH-isoBu)]$_2$ (3c). Into a screw-capped test tube was weighed 186 mg (0.201 mmol) of **1**. H_2N-isoBu (10 mL) was added to the test tube. The test tube was sealed, and the reaction was stirred at room

(62) Fitton, P.; Johnson, M. P.; McKeon, J. E. *J. Chem. Soc., Chem. Commun.* **1968**, 6−7.

temperature for 1 h, over which time the reaction mixture became homogeneous. A $^{31}P\{^1H\}$ NMR spectrum of the reaction mixture indicated complete consumption of the starting material. The reaction mixture was filtered through Celite, concentrated, and layered with Et_2O. The THF/Et_2O solution was cooled at −35 °C to yield 121 mg (61.5%) of white crystalline material. ^1H NMR (C_6D_6): δ −0.6 (m, 2H), 0.13 (d, J = 6.3 Hz, 6H), 0.68 (d, J = 6.6 Hz, 6H), 1.83 (m, J = 4.0 Hz, 2H), 2.63 (m, J = 3.8 Hz, 2H), 3.62 (m, 2H), 6.83−7.07 (m, 24H), 7.52−7.69 (m, 16H). $^{31}P\{^1H\}$ NMR (THF) δ 29.4. $^{13}C\{^1H\}$ NMR (C_6D_6): δ 20.0 (s), 21.4 (s), 34.3 (s), 60.9 (s), 122.1 (s), 126.9 (s), 128.5 (apparent t, J = 4.6 Hz), 129.9 (s), 132.7 (d, J = 42.2 Hz), 134.6 (apparent t, J = 6.0 Hz), 138.3 (s), 157.2 (d, J = 11.0 Hz). IR (cm^{-1}, KBr): 3336 (w, ν_{NH}), 3304 (w, ν_{NH}). Anal. Calcd for $C_{56}H_{60}N_2P_2Pd_2$: C, 64.93; H, 5.84; N, 2.70. Found: C, 64.64; H, 5.89; N, 2.67.

Preparation of *trans*-$(PPh_3)_2Pd(C_6H_5)(NC_4H_4)$ (4). Into a vial was weighed 120 mg (0.130 mmol) of **1** with 170 mg (0.649 mmol) of PPh_3. The solids were dissolved in 8 mL of THF and 45 μL (0.649 mmol) of pyrrole. The reaction was stirred for 2 h. The $^{31}P\{^1H\}$ spectrum indicated complete consumption of the starting material. The reaction solution was filtered through Celite, concentrated, and layered with Et_2O. Cooling the THF/Et_2O solution at −35 °C gave 183 mg (91%) of light orange crystals. ^1H NMR (C_6D_6): δ 6.36−6.48 (m, 3H), 6.52 (m, 2H), 6.65 (m, 2H), 6.91−7.05 (m, 18H), 7.11 (d, J = 7.0 Hz, 2H), 7.31−7.38 (m, 12H). $^{31}P\{^1H\}$ NMR (THF): δ 20.6. Anal. Calcd for $C_{46}H_{39}NP_2Pd$: C, 71.37; H, 5.08; N, 1.81. Found: C, 71.13; H, 5.01; N, 1.77.

Preparation of *syn*-$[(PPh_3)(p\text{-}CH_3C_6H_4)Pd(\mu\text{-}S\text{-}t\text{-}Bu)]_2$ (5). Into a screw-capped test tube was weighed 100 mg (0.10 mmol) of $[(PPh_3)(p\text{-}CH_3C_6H_4)Pd(\mu\text{-}OH)]_2$. The solid material was dissolved in 8 mL of THF, and HS-*t*-Bu (21 mg, 0.24 mmol) was added to the test tube. The test tube was sealed, and the reaction was stirred at room temperature for 1 h. The reaction mixture turned dark red. A $^{31}P\{^1H\}$ NMR spectrum of the reaction mixture indicated complete consumption of the starting material. The reaction mixture was filtered through Celite, concentrated, and layered with Et_2O. The THF/Et_2O solution was cooled at −35 °C to yield 56 mg (49%) of white crystalline material. ^1H NMR (C_6D_6): δ 1.21 (s, 9H), 1.47 (s, 9H), 2.05 (s, 6H), 6.62 (d, J = 7.4 Hz, 4H), 6.94−7.05 (m, 18H), 7.53 (d, J = 7.4 Hz, 4H), 7.62−7.68 (m, 12H). $^{13}C\{^1H\}$ NMR (C_6D_6): δ 20.8 (s), 34.6 (s), 38.3 (s), 45.5 (s), 47.7 (s), 127.9 (t, J = 4.7 Hz), 129.5 (s), 131.1 (s), 133.0 (d, J = 43.6 Hz), 135.2 (t, J = 5.3 Hz), 139.6 (s), 147.3 (t, J = 3.0 Hz). $^{31}P\{^1H\}$ NMR (THF): δ 21.8.

Variable-Temperature Determination of K_{eq} for Reaction of 1 with $H_2NC_6H_5$. Complex **1** (18.1 mg, 0.020 mmol) was dissolved in 0.5 mL of a mixture of THF with a small amount of toluene-d_8 and transferred to a screw-capped NMR tube containing a PTFE septum. H_2NPh (1.8 μL, 0.020 mmol) and H_20 (8.8 μL, 0.49 mmol) were added to the NMR tube by syringe. The NMR tube was placed into the NMR probe cooled at −20 °C, and the sample was shimmed. $^{31}P\{^1H\}$ NMR spectra were taken at 10 °C intervals up to 40 °C. The sample was allowed to equilibrate for a minimum of 40 min and was reshimmed at each temperature before data were acquired. $^{31}P\{^1H\}$ NMR spectra were acquired with a minimum 30 s pulse delay (T_1 = 3.6 s for **1**).

Measurement of K_{eq} for Reaction of 1 with H_2N-*sec*-Bu. Complex **1** (11 mg, 0.012 mmol) was weighed into a small vial along with a small amount (<2 mg) of trimethoxybenzene to act as an internal standard. The solids were dissolved in 0.6 mL of anhydrous THF-d_8 and transferred to a screw-capped NMR tube. The NMR tube was sealed with a cap containing a PTFE septum and removed from the drybox. A ^1H NMR spectrum was taken. Water (5.0 μL, 0.28 mmol) and H_2N-*sec*-Bu (2.4 μL, 0.024 mmol) were added to the NMR tube by syringe. The reaction was left at room temperature for 12 h. The equilibrium concentrations were determined by integration of the ^1H NMR spectrum. K_{eq} was calculated to be 12.

Kinetic Analysis of the Reaction of 1 with H_2N-*sec*-Bu. *Dependence on [H_2N-sec-Bu]:* $[(PPh_3)(C_6H_5)Pd(\mu\text{-}OH)]_2$ was weighed into a vial (21.7 mg or 50.3 mg) and dissolved in THF-d_8 (1.3 mL or 1.8 mL). An aliquot of the standard solutions (0.50 and 0.45 mL) was placed into a screw-capped NMR tube. The tube was sealed with a cap containing a PTFE septum and removed from the drybox. The appropriate amount of H_2N-*sec*-Bu (4.5−20.5 μL) was added to the NMR tube by syringe right before data acquisition began. Reaction rates were monitored by ^1H NMR spectroscopy at 25 °C using an automated program that collected single-pulse experiments with at least 1 min intervals between data acquisitions. The resonance for the hydroxyl proton and an aromatic resonance were used to monitor the concentration of **1** throughout the course of the reaction. The following pseudo-first-order rate constants were obtained at different concentrations of H_2N-*sec*-Bu (k, [H_2N-*sec*-Bu]): 4.3×10^{-5} s^{-1}, 0.089 M; 1.2×10^{-4} s^{-1}, 0.15 M; 3.1×10^{-4} s^{-1}, 0.27 M; 4.3×10^{-4} s^{-1}, 0.30 M; 1.2×10^{-3} s^{-1}, 0.45 M.

Dependence on [H_2O]: $[(PPh_3)(C_6H_5)Pd(\mu\text{-}OH)]_2$ was weighed into a vial (41.2 mg, 0.0446 mmol) and dissolved in 2.5 mL of THF-d_8. A 0.56 mL aliquot of the standard solution was placed into a screw-capped NMR tube. The tube was sealed with a cap containing a PTFE septum and removed from the drybox. H_2N-*sec*-Bu (10 μL, 0.10 mmol) and the appropriate amount of H_2O (3−14 μL) were added to the NMR tube by syringe right before data acquisition began. Data were acquired as described above. The following pseudo-first-order rate constants were obtained at different concentrations of H_2O (k, [H_2O]): 7.4×10^{-4} s^{-1}, 0.30 M; 6.6×10^{-4} s^{-1}, 0.49 M; 4.8×10^{-4} s^{-1}, 0.69 M; 3.9×10^{-4} s^{-1}, 0.88 M; 3.5×10^{-4} s^{-1}, 1.0 M; 3.0×10^{-4} s^{-1}, 1.4 M.

Synthesis of D_2N-*sec*-Bu: H_2N-*sec*-Bu (8 mL) was placed into a 25 mL screw-capped test tube. D_2O (8 mL) was added to the test tube. The mixture was shaken vigorously. Enough NaCl was added to the tube to saturate the D_2O, and the amine was extracted with n-Bu_2O (2 × 5 mL). The ether layer was then mixed with additional D_2O (2 × 5 mL). The ether layer was then collected, and the deuterated amine was isolated by distillation under N_2(g). A ^1H NMR spectrum of the amine showed no resonance for the amino protons.

Synthesis of $[(PPh_3)(C_6H_5)Pd(\mu\text{-}OD)]_2$. $[(PPh_3)(C_6H_5)Pd(\mu\text{-}OH)]_2$ (125 mg) was weighed into a 20 mL vial and dissolved in 5 mL of THF. D_2O (10 mL) was added to the vial. The mixture was stirred for 8 h. The product was collected on a medium-fritted funnel. The ^1H NMR spectrum showed no resonance for the hydroxo protons.

Measurement of Isotope Effect for the Reaction of $[(PPh_3)(C_6H_5)Pd(\mu\text{-}OD)]_2$ with D_2N-*sec*-Bu. **1**-μ-$(OD)_2$ (5.8 mg, 0.0063 mmol) was weighed into a small vial and dissolved in 0.45 mL of THF-d_8. This solution was transferred to a screw-capped NMR tube. The tube was sealed with a cap containing a PTFE septum and removed from the drybox. D_2N-*sec*-Bu (15 μL of a 5.2 M solution in n-Bu_2O, 0.078 mmol) was added to the NMR tube by syringe. Data were collected as described above. The psuedo-first order-rate constant obtained were 1.9×10^{-4} and 2.1×10^{-4} s^{-1} resulting in k_H/k_D = 0.7 ±.1.

Reaction of 3a with H_2O. 3a (8.6 mg, 0.0088 mmol) was weighed into a small vial and dissolved in 0.5 mL of THF. The solution was transferred to a screw-capped NMR tube. The tube was sealed with a cap containing a PTFE septum and removed from the drybox. H_2O (16 μL, 0.89 mmol) was added to the reaction by syringe. The NMR tube was heated at 70 °C for 1.5 h. The $^{31}P\{^1H\}$ NMR spectrum indicated complete conversion to **1**.

Kinetic Analysis of the Reaction of 3b with H_2O. *Dependence on [H_2N-sec-Bu]:* Complex **3b** (30.4 mg, 0.0311 mmol) was dissolved in 2.5 mL of THF-d_8. A 0.50 mL aliquot of the stock solution was placed in a screw-capped NMR tube. The tube was sealed with a cap containing a PTFE septum and removed from the drybox. D_2O (110 μL, 5.50 mmol) and

the appropriate amount of H_2N-*sec*-Bu (3.1−18.5 μL) were added to the NMR tube by syringe right before data acquisition began. Reaction rates were monitored by ^1H NMR spectroscopy at 70 °C. Data were acquired as described above. The following pseudo-first-order rate constants were obtained at different concentrations of H_2N-*sec*-Bu (k, [H_2N-*sec*-Bu]): 5.2×10^{-4} s^{-1}, 0.050 M; 7.8×10^{-4} s^{-1}, 0.075 M; 7.7×10^{-4} s^{-1}, 0.099 M; 1.0×10^{-4} s^{-1}, 0.12 M; 1.4×10^{-3} s^{-1}, 0.15 M; 1.3×10^{-3} s^{-1}, 0.17 M; 1.5×10^{-3} s^{-1}, 0.20 M; 2.2×10^{-3} s^{-1}, 0.25 M; 3.3×10^{-3} s^{-1}, 0.29 M.

Dependence on [H_2O]: 3b (28.4 mg, 0.0290 mmol) was dissolved in 2.0 mL of THF-d_8. A 0.40 mL aliquot of the stock solution was placed in a screw-capped NMR tube. The tube was sealed with a cap containing a PTFE septum and removed from the drybox. H_2N-*sec*-Bu (5.8 μL, 0.057 mmol) and the appropriate amount of D_2O (68−137 μL) were added to the NMR tube by syringe right before data acquisition began. Reaction rates were monitored by ^1H NMR spectroscopy at 70 °C. Data were acquired as described above. The following pseudo-first-order rate constants were obtained at different concentrations of H_2O (k, [H_2O]): 1.6×10^{-3} s^{-1}, 7.31 M; 1.6×10^{-3} s^{-1}, 10.2 M; 1.7×10^{-3} s^{-1}, 12.7 M.

Autocatalytic Behavior: 3b (19.8 mg, 0.0202 mmol) was dissolved in 0.50 mL of THF-d_8 and transferred into an NMR screw-capped NMR tube sealed with a cap containing a PTFE septum. The NMR tube was removed from the drybox, and 10.0 μL (0.500 mmol) of D_2O was added to the tube by syringe. The reaction was monitored by ^1H NMR spectroscopy at 70 °C. Data were acquired as described above.

Acknowledgment. This work was generously supported by the Department of Energy (Grant No. DE-RG02-96ER14678). We also gratefully acknowledge support from a DuPont Young Professor Award, a Union Carbide Innovative Recognition Award, a National Science Foundation Young Investigator Award, a Dreyfus Foundation New Faculty Award, and a Camile Dreyfus Teacher-Scholar Award for support for this work. J.F.H. is a fellow of the Alfred P. Sloan Foundation. We thank Alpha/Aesar for donation of palladium chloride.

Supporting Information Available: Plots of kinetic data for the reaction of *sec*-butylamine with **1** and the reaction of **3b** with H_2O and *sec*-butylamine (3 pages). Ordering information is given on any current masthead page.

OM970856L